15th World Congress on Computational Mechanics (WCCM-XV)
8th Asian Pacific Congress on Computational Mechanics (APCOM-VIII)
Virtual Congress: 31 July – 5 August 2022
S. Koshizuka (Ed.)

ASSESSMENT OF MACRO AND MICRO LEVEL HETEROGENEITIES FOR CHARACTERIZING MECHANICAL BEHAVIOR OF SAND IN BIAXIAL TEST EMPLOYING DEM

MADHU S. NEGI[1] AND MOUSUMI MUKHERJEE[2]

[1] Research Scholar
Indian Institute of Technology Mandi, India
d20013@students.iitmandi.ac.in

[2] Assistant Professor
Indian Institute of Technology Mandi, India
mousumi@iitmandi.ac.in

Key words: Macro and micro level heterogeneity, Biaxial test, Representative area element (RAE), Wall-based measurement

Abstract. *While characterizing the mechanical behavior of granular assemblies through DEM simulations, various macro and micro level heterogeneities are often encountered. Such macro level heterogeneities may arise due to stress and void concentration near the wall boundaries; whereas, the micro level heterogeneities are attributed to consideration of only limited number of particles within the representative volume element (RVE). The present study assesses these macro and micro level heterogeneities in reference to the mechanical characterization of sand in DEM-based biaxial test simulation with both rigid and flexible lateral boundaries. In this regard, stresses and strains have been calculated using a wall-based global estimation and a representative area element (RAE)-based local estimation. It has been suggested that the RAE should occupy a maximum of 90% area of the specimen in order to avoid any macro level heterogeneity and can still be able to capture its overall mechanical behavior. For obtaining the spatial variation of field variables, RAE of smaller diameters are often employed. In such cases, depending on the average particle size of the granular assembly and the specimen dimensions, the diameter of the RAE should be selected ensuring that it is small enough to aptly capture the local variation of field variables and at the same time, large enough to avoid any micro level heterogeneity.*

1 INTRODUCTION

Discrete element method (DEM) is widely used to examine the mechanical behavior of granular assemblies, like sand, under various loading conditions by performing numerical simulations replicating different laboratory tests [1-7,10-12]. It can give important information about the evolution of particle displacements, rotations and orientations which are very difficult to measure in the standard laboratory experiments. While simulating various element tests, e.g., triaxial or biaxial test using such particle-based methods, it is often required to estimate quantities such as stresses and strains that are essentially defined based on a continuum assumption. In this regard, either a wall-based global estimation or a representative volume

element (RVE)-based local assessment is often adopted. Wall-based estimation predicts an overall response of the specimen, which takes into account only the particle to wall contacts. As a result, such wall-based estimation of field variables is often influenced by the boundary effects arising due to the concentration of stresses and voids around wall boundaries [3,7], which can be identified as a source for macro level heterogeneities. Whereas, RVE-based estimation considers all the particle contacts within RVE domain and is considered to be statistically representative of the specimen under consideration. Further, the RVE must be large enough so that an increase in the size will not change the estimated field variables and should exclude any possible macro level heterogeneities. In addition, an RVE should not be too small such that it starts to depict micro level heterogeneities, such as the development of unrealistic localized zones of various field variables due to consideration of a limited number of particles within the RVE [5]. However, deciding the optimal extent of the RVE to avoid such macro or micro level heterogeneities requires a systematic analysis.

In the present study, 2D-DEM-based biaxial test simulations have been performed with consideration of both rigid and flexible lateral boundaries. In this regard, circular and non-circular particles have been considered conforming to the particle size distribution of Evans et al. [2] and Tian et al. [6]. Subsequently, the influence of the macro and micro level heterogeneities on the mechanical behavior of the specimen has been assessed by selecting various configurations of representative area elements (RAE). In this reference, a series of simulations have been carried out by generating various RAE configurations with different diameter and area fraction coverage over the specimen. Further, RAE's of smaller diameters have been also employed within the specimen in order to examine the local variation of the field variable.

2 DEM MODELING OF BIAXIAL TEST

Drained biaxial test simulations have been conducted using a commercially available DEM code, Particle Flow Code-2D, PFC^{2D} [8]. Granular sand specimens have been generated with two types of lateral boundaries, one with a velocity-controlled rigid boundary and another with a stress-controlled flexible boundary. The model geometry and material parameters for the specimen with rigid and flexible lateral boundaries are listed in Table 1, which have been adopted from Evans et al. [2] and Tian et al. [6], respectively. Figure 1 presents the particle size distribution for both these cases. The specimen with the rigid lateral boundary has been composed of non-circular clumped particles with a mean particle diameter, d_{50} = 5 mm and an aspect ratio (AR = longest dimension/shortest dimension) of 1.5. Whereas, the specimen with flexible lateral boundary has been made of circular particles with d_{50} = 0.993 mm and AR = 1. The biaxial test simulations have been performed in three steps, namely, particle generation, isotropic compression and biaxial shearing stage. In the particle generation stage, the particles have been generated in a larger domain in order to ensure no overlap takes place between the particles. In the subsequent isotropic compression stage, the boundary walls have been moved inward until the required confining stress has been achieved. Finally, in the biaxial shearing stage, the specimens have been compressed vertically with the strain-controlled top and bottom platen. During this stage, the confining pressure on the specimen has been maintained constant using either a velocity-controlled rigid boundary or a stress-controlled flexible lateral boundary. In both the cases, a linear elastic type contact model has been implemented for representing the

normal and shear interaction between the particles and a Coulomb friction law has been employed for defining the maximum shear force allowed at the particle contact.

Table 1: Model geometry and material properties

Parameter	Magnitude	
	Rigid lateral boundary [2]	Flexible lateral boundary [6]
Initial specimen height (mm)	180	100
Initial specimen width (mm)	90	50
Porosity before shearing	0.076	0.152
Particle and platen properties		
Particle density (kg/m^3)	2650	2630
Particle/platen normal stiffness (N/m)	1x10^8	1.5× 10^8
Particle/platen shear stiffness (N/m)	1x10^7	1× 10^8
Particle friction coefficient	0.31	0.5
Wall properties		
Wall normal stiffness (N/m)	1x10^7	-
Wall shear stiffness (N/m)	1x10^6	-
Membrane properties		
Normal bond strength (Pa)	-	1× 10^{300}
Shear bond strength (Pa)	-	1.5× 10^{300}
Normal contact stiffness (N/m)	-	1× 10^6
Shear contact stiffness (N/m)	-	1× 10^6
Shearing parameters		
Confining pressure (kPa)	150	200
Axial strain rate -SR (/s)	0.55	0.5

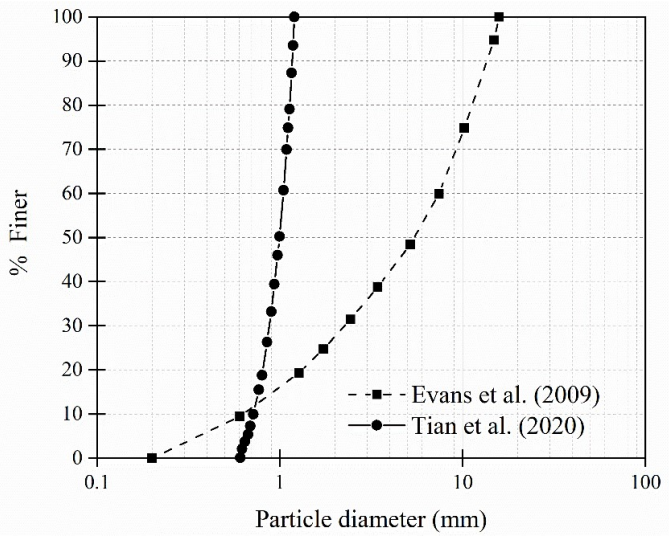

Figure 1: Particle size distribution

The DEM code has been verified first by comparing the macro level stress-strain and volumetric predictions from the biaxial test simulation against the results reported in Evans et al. [2] and Tian et al. [6]. It is to be noted that Evans et al. [2] reported an axial strain rate, SR = 0.0055 /s in their study. Hence, in the verification study for specimen with rigid lateral boundary a low axial strain rate of SR = 0.0055 /s has been adopted, which lead to significant increase in the computational time. In order to increase the computational efficiency, an additional simulation with SR = 0.55 /s has also been carried out for this specimen. Figure 2 presents the simulated stress-strain and volumetric responses of the specimen along with a comparison against Evans et al. [2]. The stress-strain and volumetric behavior of the specimen matches well with the verification study at the lower strain level; however, minor variations can be observed at the higher strain level that might be attributed to the difference in the initial particle packing arrangement. It is observed from Figures 2(a) and (b) that there exists a negligible effect of employed higher axial strain rate on the stress-strain and volumetric behavior of the specimen. This might be due to the existence of a quasistatic condition at the chosen ranges of axial strain rate, which has been further verified by checking the inertial number, I calculated from the following equation

$$I = \dot{\varepsilon}_a \sqrt{\frac{m}{p}} \tag{1}$$

where, $\dot{\varepsilon}_a$ is the axial strain rate, m is the mass of the particle and p is the mean stress. It can be observed from Figure 2(c) that the inertial number for the chosen higher axial strain rate is less than 10^{-3}, which is often considered as a threshold for the quasistatic regime [9]. Hence, SR = 0.55 /s has been adopted for rest of the simulations with rigid lateral boundary.

The stress-strain and volumetric response for the specimen with flexible lateral boundary have been depicted in Figure 3. It is to be noted that the specimen with flexible lateral boundary exhibits a non-homogeneous localized deformation pattern within the specimen i.e., the formation of shear band, which was also reported in the verification study of Tian et al. [6]. Though the overall mechanical response gives a reasonable match with that of Tian et al. [6], small deviations in the stress-strain and volumetric response can be noticed due to difference in the particle arrangements and configuration of the shear band.

Both the specimens with rigid and flexible lateral boundaries depict a typical stress-strain response of dense sand as observed in the laboratory experiments, i.e., an initially increasing stress deviator with a distinct peak, which is then followed by a softening response reaching to a residual stress at large strain level. On the contrary, the volumetric strain decreases at first indicating an initial compression and then increases continuously exhibiting a dilative response till the critical state has been reached at the large strain level.

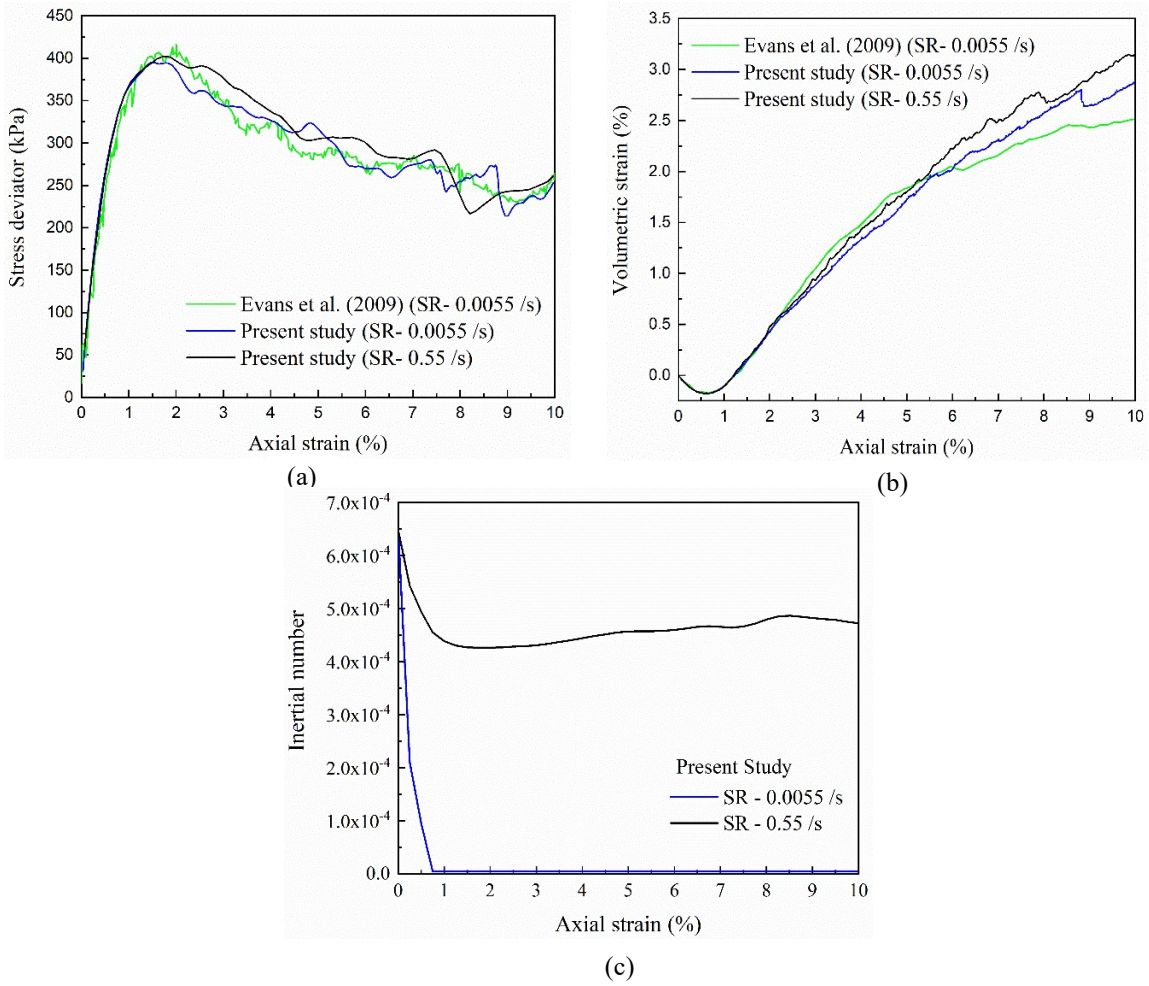

Figure 2: Evolution of (a) stress-strain, (b) volumetric response and (c) inertial number with shearing for the biaxial simulation with rigid lateral boundary.

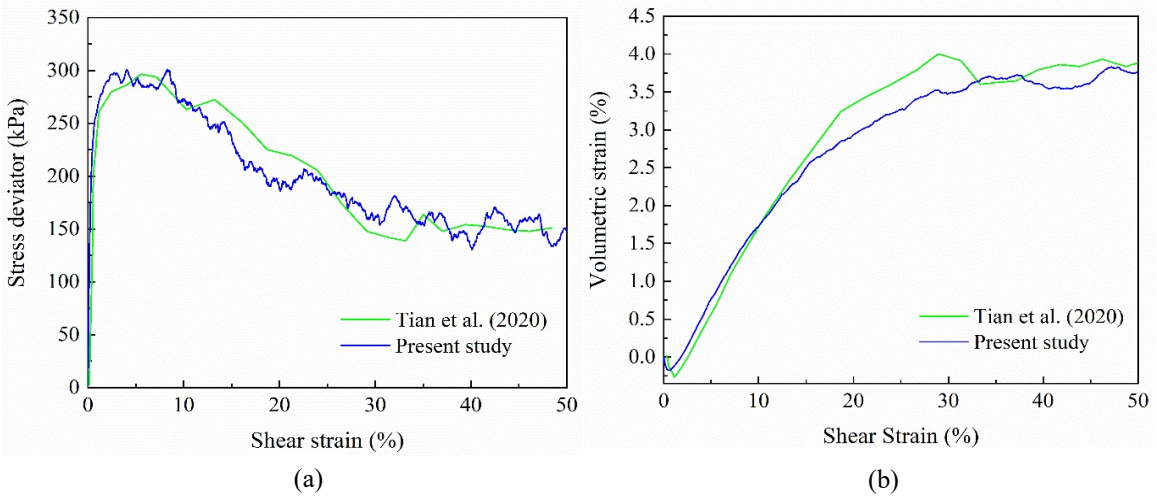

Figure 3: Evolution of (a) stress-strain and (b) volumetric response with shearing for the biaxial simulation with flexible lateral boundary.

3 MACRO LEVEL HETEROGENEITY CHARACTERIZATION

The continuum-based field quantities such as stresses and strains have been calculated from either a wall-based global estimate or a representative area element (RAE)-based local assessment. The wall-based stresses (σ_k^W) have been estimated based on the average contact force exerted on the opposite walls and the corresponding cross-sectional area as given below

$$\sigma_k^W = \frac{\frac{1}{2}\left((F_k^W)^L + (F_k^W)^R\right)}{A_k}, \quad k = \{x, y\} \tag{2}$$

where $(F_k^W)^L$ and $(F_k^W)^R$ are the total forces on the left and right walls in the k^{th} direction respectively, and A_k is the specimen cross-sectional area perpendicular to the k^{th} direction. The wall-based strain quantities have been determined from the changed distance between the opposite walls

$$\varepsilon_k^W = \frac{d_k^W - (d_k^W)_0}{(d_k^W)_0}, \quad k = \{x, y\} \tag{3}$$

where d_k^W is the distance between opposite walls in k^{th} direction , and $(d_k^W)_0$ is the initial distance between these walls.

On the contrary, representative area element (RAE)-based stresses have been estimated as the average stress σ^M within a measurement region of area A_m

$$\sigma^M = \frac{1}{A_m}\sum_{N_c} F^{(c)} \otimes L^{(c)} \tag{4}$$

where N_c is the number of particle contacts within the measurement region, $F^{(c)}$ is the contact force vector, $L^{(c)}$ is the branch vector joining the centroids of the two particles in contact and the symbol $\otimes$ denotes outer product. The RAE-based strains have been calculated following a best-fit procedure that minimizes the fluctuation of velocities for all the particles contained within the measurement region in reference to the average estimated velocity. The detail calculation of RAE-based stresses and strains can be found in Potyondy and Cundall [1].

Conventionally, in biaxial test simulations following DEM, RAE-based stresses and strains are calculated from the average value of the three measurement circles of fixed diameter (D), which is related to the initial width ($W_{initial}$) of the specimen (Figure 4a) [6,8]. Due to such assumption of fixed diameter, the measurement circles might overlap with the specimen boundary during the continued deformation at higher strain level, which may lead to an erroneous estimation of stress and strain. In order to overcome this problem, the present study adopts a concept of evolving diameter of the measurement unit, which depends on the current width (W) of the specimen and hence, maintains a constant area coverage in reference to the deformed configuration of the specimen. In this regard, various configurations of measurement circles with different D/W ratios have been employed to determine the stress-strain response of the specimen. The same has been depicted in Figure 4 along with a fixed diameter measurement circle for the specimen with rigid boundary at 0 % and 20 % global axial strain levels.

Figure 5 depicts the effect of increasing D/W ratio of the measurement circle on the stress-strain and volumetric response of the specimen with rigid lateral boundary. It can be observed from Figure 5(a) that the wall-based estimation leads to higher stresses as compared to the stresses obtained from the measurement circle-based analysis due to stress concentration near the wall boundaries [7]. It is to be also noted that increasing the extent of the measurement

circle leads to a higher estimation of the stresses, which also becomes comparable to the wall-based stress estimates. This further confirms the existence of stresses concentration near the wall boundaries. It is therefore suggested that the RAE should occupy a maximum of 90% volume of the specimen in order to avoid any possible boundary effects and can still capture the overall mechanical response of the specimen. Further, it has also been observed that the wall-based estimation results in unrealistically large volumetric dilation at higher strain levels and subsequently hinders the possibility to attain the critical state in the simulation (Figure 5b). In comparison to the wall-based estimation, the measurement circle-based volumetric predictions exhibit lesser dilation at any strain level and achieves a constant volumetric strain at larger strain level. While comparing the measurement circle-based stress-strain estimations, it can be clearly noticed that after 8 % global axial strain level, the specimen shows no change in the volumetric strain and the corresponding stress deviator also remains constant. These observations confirm the attainment of critical state conditions in the specimen at higher strain level, which has not been observed from the wall-based estimation. It has been also observed that increasing the extent of measurement circle results into prediction of a lesser dilative behavior.

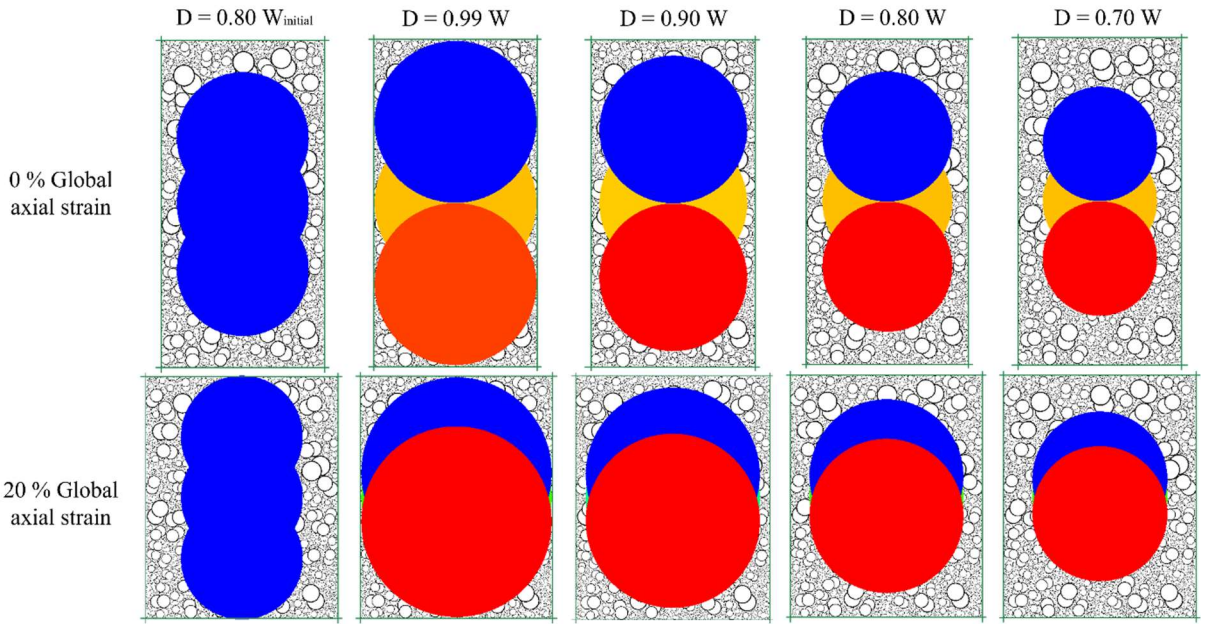

Figure 4: Measurement circle configurations for rigid lateral boundary, where *D* and *W* are the diameter of measurement circle and specimen width, respectively.

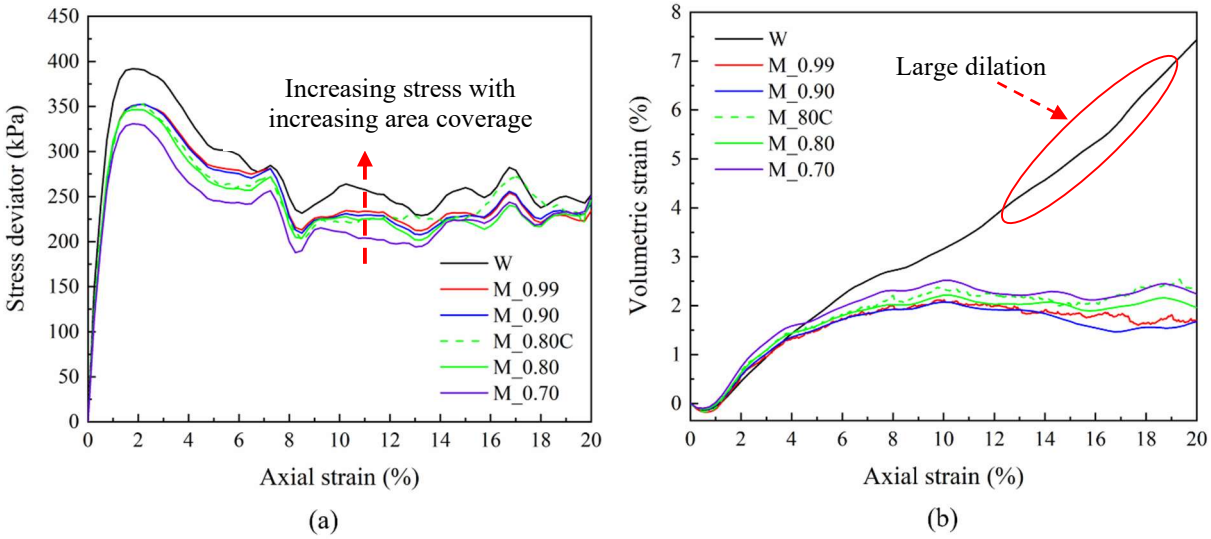

Figure 5: Influence of measurement circle configurations on the (a) stress-strain and (b) volumetric response of specimen with rigid lateral boundary.

The effect of increasing *D/W* ratio of the measurement circle on the stress-strain-volumetric prediction of the specimen with flexible lateral boundary has been presented in Figure 6. It can be observed that increasing the extent of the measurement circle does not incur significant changes in the estimated stress and volumetric strain magnitudes at lower strain level. This clearly indicates that the macro level heterogeneity is not that significant for the specimens with flexible lateral boundary at these strain levels. However, the stresses and strains can be noticed to be overestimated when the measurement circle configuration with a smaller *D/W* ratio (i.e., M_0.70) has been employed. This might be attributed to the formation of cross-type shear band which passes through the center of the specimen. Buckling of force chains has been observed in the shear band region, which resulted due to formation of strong force chain network near the center of the specimen. Significant volumetric dilation has also been observed near to these zones. Hence, estimation of the stresses and strains by only considering the central region can affect the accuracy of the results. Therefore, it is recommended that the size of the measurement circle should be sufficiently large to capture the representative stress and strain magnitude for the complete specimen.

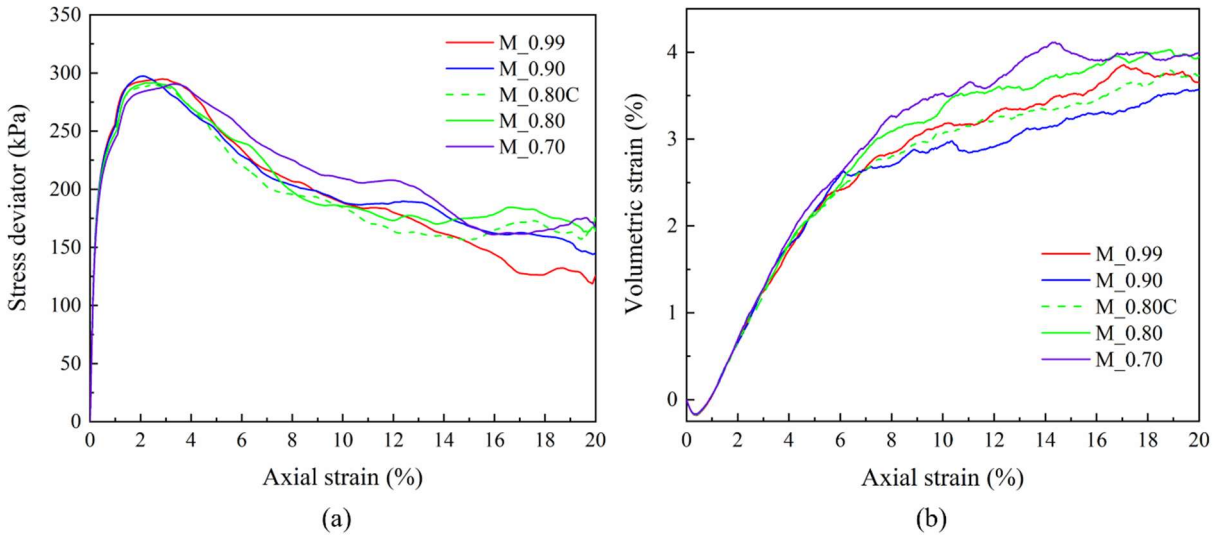

Figure 6: Influence of measurement circle configurations on the (a) stress-strain and (b) volumetric response of specimen with flexible lateral boundary.

4. MICRO LEVEL HETEROGENEITY CHARACTERIZATION

While examining the local variations of field variables within the specimen domain, RAE of smaller diameters are often adopted [4-5,10-12]. For such cases, the size of the RAE needs to be selected such that it should not be too large to average out the local variation of the field variable. At the same time, it should not be too small to depict the micro level heterogeneities, i.e., the development of unrealistic localized zones of various field variables due to consideration of only limited number of particles within the RAE. In order to decide the optimum size of the RAE, measurement circles of various smaller diameters have been considered for specimens with both types of lateral boundary conditions. The D/d_{50} ratio has been varied to obtain the representative porosity field within the specimen. In this regard, the measurement circle configurations with two typical D/d_{50} values have been presented in Figure 7 for both the lateral boundary cases at 20 % global axial strain level. The porosity has been further calculated based on the total area of particles within a measurement circle and the area of the measuring circle itself. Thus calculated porosity values have been then assigned at the center of the measurement circle for representing the spatial variation of the porosity field within the specimen.

The spatial variation of porosity at 20 % global axial strain level has been presented in Figure 8 with various D/d_{50} ratios for both the lateral boundary cases. It can be observed that with an increasing D/d_{50} ratio, the spatial variation in the porosity field becomes less evident due to the reduced number of representative data points within the specimen. On the contrary, the selection of a small D/d_{50} ratio leads to the development of various localized regions of porosity field due to consideration of only limited number of particles within the RAE. In order to obtain presentative values of the field variable, various researchers have suggested that the number of particles inside the measurement circle should be more than 200 [5-6] or D/d_{50} has to be taken in the range of 10-12 [4,10-12]. In the present study, since the d_{50} value itself is quite large (i.e., 5 mm) for the specimen with rigid lateral boundary, the spatial variation of porosity field

becomes distinct when an RAE configuration of D/d_{50} = 3.46 has been selected. Whereas, for the specimen with the flexible lateral boundary and comprising of particles smaller d_{50} (i.e., 0.993 mm), the spatial variation of porosity becomes evident while analyzing with an RAE configuration of D/d_{50} = 6.50. It is to be noted that the specimen with rigid lateral boundary has W/d_{50} ratio of 18; whereas, the specimen with flexible lateral boundary has W/d_{50} = 50. Which indicates that, for a larger W/d_{50} ratio, the D/d_{50} ratio required for distinct spatial representation of field variable is also large. Hence, it can be inferred that the representation of spatial variation of field variables not only depends on d_{50} of the particles but the specimen dimensions i.e., W also play an important role in deciding the optimal diameter of the RAE which requires further study.

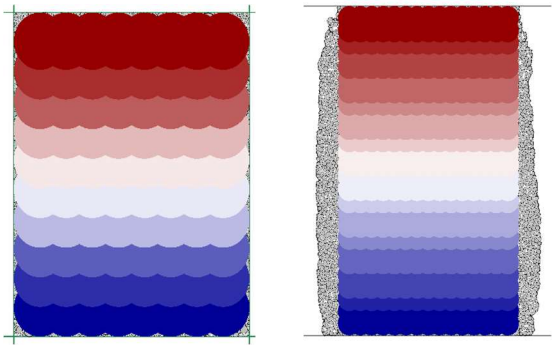

Figure 7: Measurement circle configurations at 20 % global axial strain for (a) rigid lateral boundary with D/d_{50} = 3.46 and (b) flexible lateral boundary with D/d_{50} = 6.50.

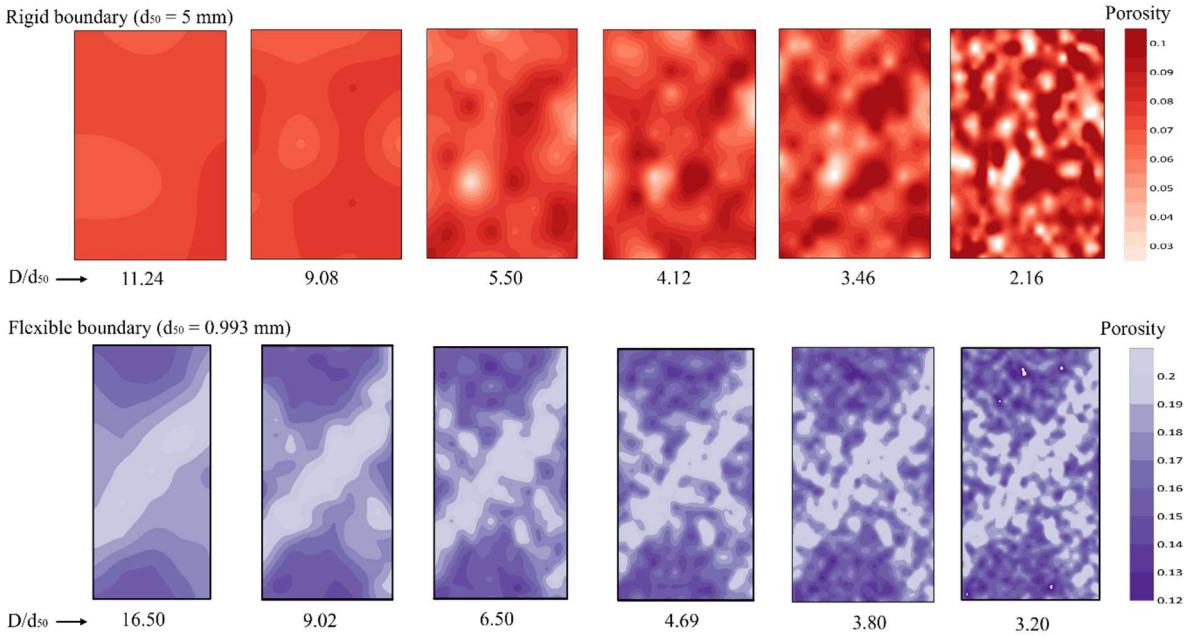

Figure 8: Porosity variation at 20 % global axial strain level for specimen with (a) rigid lateral boundary (b) flexible lateral boundary.

5 CONCLUSION

The present study analyzes the macro and micro level heterogeneities that arise in the mechanical characterization of a granular sand specimen in element level test. In this regard, biaxial test simulations have been conducted employing two different lateral boundaries i.e., rigid and flexible. The macro level heterogeneities have been assessed in terms of stresses and strains, which have been calculated from a global wall-based and local RAE-based estimation. The micro level heterogeneities have been assessed from the local porosity variation within the specimen estimated using RAE's of smaller diameter. The major conclusions inferred from the DEM study are listed below:

- For accurate estimation of field quantities, the RAE should evolve with continued deformation in order to ensure a constant area coverage in reference to the deformed configuration of the specimen.
- In the case of simulations with rigid lateral boundaries, wall-based estimation predicts higher stresses and increasing the extent of RAE predicts stresses in the range of wall-based measurements due to the concentration of stresses near wall boundaries. Hence, the RAE should occupy a maximum of 90% area of the specimen to avoid any possible boundary effects.
- In the case of simulations with flexible lateral boundaries, macro level heterogeneity is insignificant since there is no concentration of stresses near the boundaries; however, the size of the RAE should be sufficiently large to capture the representative stress and strain magnitude for the complete specimen.
- In order to capture the local variation of field variables, the diameter of the RAE should be selected ensuring that it is small enough to aptly capture the local variation of field variables and at the same time, large enough to avoid any micro level heterogeneity. In this regard, the selection of optimal RAE diameter, D for representing the spatial variation of the field variables is not only guided by d_{50} of the particles but the specimen dimensions also play an important role, which requires further study.

ACKNOWLEDGEMENT

The authors would like to acknowledge the support rendered by Dr. Arghya Das from Indian Institute of Technology Kanpur, India for granting access to the PFC 2D software.

REFERENCES

[1] Potyondy, D. O. and Cundall P. A. A bonded-particle model for rock. International Journal of Rock Mechanics and Mining Sciences (2004) **41**(8):1329–1364.

[2] Evans, T. M., Mojarrad, H., Cunningham, C. and Tayebali A. A. Grain Size Distribution Effects in 2D Discrete Numerical Experiments. Contemporary topics in situ testing, analysis, and reliability of foundation. Geotechnical special publication (2009) **185**:58–65.

[3] Huang, X., Hanley, K. J., O'Sullivan, C. and Kwok, F. C. Y. Effect of sample size on the response of DEM samples with a realistic grading. Particuology (2014) **15**:107–115.

[4] Jiang, M., Yin, Z. Y. and Shen, Z. Shear band formation in lunar regolith by discrete element analyses. Granular Matter (2016) **18**(2):1–14.

[5] Lü, X., Zeng, S., Li, L., Qian, J. and Huang, M. Two-dimensional discrete element simulation of the mechanical behavior and strain localization of anisotropic dense sands. Granular Matter (2019) **21**(2):1–16.
[6] Tian, J., Liu, E. and He, C. Shear band analysis of granular materials considering effects of particle shape. Acta Mechanica (2020) **231**(11):4445–4461.
[7] Cheung, G. and O'Sullivan, C. Effective simulation of flexible lateral boundaries in two- and three-dimensional DEM simulations. Particuology (2008) **6**(6):483–500.
[8] Itasca Consulting Group, Inc. PFC—Particle Flow Code, Ver. 5.0. (2014) Minneapolis.
[9] Midi, G. D. R. On dense granular flows. European Physical Journal E (2004) **14**(4): 341–365.
[10] Jiang, M., Zhu, H. and Li, X. Strain localization analyses of idealized sands in biaxial tests by distinct element method. Frontiers of Architecture and Civil Engineering in China (2010) **4(**2):208–222.
[11] Jiang, M. J., Yan, H. B., Zhu H. H., and Utili S. Modeling shear behavior and strain localization in cemented sands by two-dimensional distinct element method analyses. Computers and Geotechnics (2011) **38(**1):14–29.
[12] Gu, X., Huang, M., and Qian, J. Discrete element modeling of shear band in granular materials. Theoretical and Applied Fracture Mechanics (2014) **72**(1):37–49.